NUMERICAL SIMULATION OF THERMAL PERFORMANCE OF COLD PLATES FOR HIGH HEAT FLUX ELECTRONICS COOLING

Hanlin Song [1], Meng Zheng [1], Zheshu Ma [1,*], Yanju Li [1], and Wei Shao [1]

[1]College of Automobile and Traffic Engineering, Nanjing Forestry University, Nanjing 210037, China.

[*] Corresponding author; E-mail: mazheshu@njfu.edu.cn

High heat flow density electronic components need cooling plates with strong heat exchange capacity to maintain temperature balance. To obtain better cooling performance, four different flow channel types of cooling plates are designed, including an S-type channel, Z-type channel, mosaic channel and double-layer channel. The maximum temperature of the cooling plate, outlet temperature and pressure drop under different working conditions and coolant are analyzed by numerical simulation. The simulation results show that the double-layer channel design can effectively enhance the heat transfer effect of the cooling plate and reduce the pressure drop. The maximum temperature of the cooling plate of the double-layer flow channel is 6.88 °C lower than that of the Z-type flow channel. Moreover, increasing the inlet flow rate and lowering the coolant inlet temperature can improve the cooling performance of the cold plate, but increasing the inlet flow rate will lead to an increase in the pressure loss of the cold plate. When the coolant of the double-layer channel cooling plate is 20% ethylene glycol-water solution, the cooling performance is better than the other three coolants. Other channel cooling plates perform better with water as the coolant.

Keywords: *Heat dissipation; Cold plate; Fluid-solid coupled heat transfer; Flow channel*

1. Introduction

With the rapid development of the economy and industrialization in modern society, environmental and ecological problems have become increasingly serious [1, 2]. To solve the problems of global warming, electronic pollution and soil pollution, it is essential to use renewable resources efficiently and transform them into green and renewable products that are competitive in the market [3-5]. As current density increases and operating frequency accelerates, electronic systems generate more and more heat. The life of electronic products can be improved through thermal management and other technical means, which can reduce electronic pollution. For example, since the radar system is equipped with a large number of the transmit and receive (T/R) modules with high heat flow density, the radar will generate a large amount of heat, so it is crucial to use a reasonable thermal

management solution to keep the overall system performance stable. While the active phased array T/R module requires high power, high efficiency and low noise, its volume should be as small as possible and its weight should be as light as possible. The demand has led to a continued move toward miniaturization and lightness in the core modules of the Radar-T/R module, which will result in elevated thermal dissipation of T/R modules with local heat flow densities exceeding 1000 W/cm2 [6]. Therefore, it is a challenge to provide reasonable and effective heat dissipation for these high-power devices to improve their reliability. If there is no proper heat dissipation mechanism, the internal temperature of the system will rise sharply, which may damage the electronic components and affect the reliability of the system [7]. Existing research shows that the main reason for 55% of the failure of electronic equipment is that a large amount of heat is generated at work, which makes the temperature of the components and the surrounding environment too high. The urgent need to improve the heat dissipation capacity has promoted the development of various feasible heat dissipation technologies [8-10].

The conventional cooling system for the radar T/R module assembly is air-cooled. However, with the increase in the power of T/R modules, air cooling can no longer meet the heat dissipation requirements, and hybrid heat dissipation emerges as the times require [11, 12]. Scott et al. introduced a cooling system with a combination of closed air circulation cooling and liquid cooling (water/glycol as coolant) designed for cooling the Sampson MFR radar [13]. In the introduction of this article, the cooling system of the American AN/FPS-115 "PAVE PAWS" radar is also a combination of liquid cooling and air cooling [14]. The US radar company also uses a combination of forced liquid cooling and forced air cooling for the heat dissipation method of THAAD radar [15]. In addition, Nakagawa et al. designed a U-shaped loop heat pipe plate for heat dissipation because of the heat dissipation requirements of T/R modules with high heat flux density [16]. In view of the increasingly complex heat dissipation problem, the cooling system using liquid as the medium has attracted much attention in recent years and is considered to be one of the most effective methods for heat dissipation of electronic devices [17-20]. Agrawal et al. used liquid cooling technology to dissipate heat from the packaged T/R modules [21]. Narvaez et al. proposed to use of a liquid cooling system to dissipate heat from the THAAD radar [22]. Liquid cooling has many benefits over air cooling, such as being able to withstand higher heat flux density, enabling localized component cooling, and quieter systems [23, 24].

In the past decades, research on liquid-cooled radiators has focused on optimizing geometric parameters, channel structure and heat source layout to improve cooling performance. Esmaili et al. experimentally investigated the effect of channel structure, manifold design and heat source layout on the thermal performance of the flow channel [25]. Zhang et al. proposed a cooling method using an S-shaped cold plate structure with baffles to avoid heat concentration while increasing heat transfer [26]. The study showed that the total resistance of the heat sink with a truncated channel design was reduced by 37.5 % and the peak temperature difference was reduced by a maximum of 36.7 % compared with the heat sink with parallel straight channels [27-29]. Vinoth et al. adopted inclined fins on the trapezoidal channel radiator, using coolants of water and nanofluids to improve heat transfer efficiency [30]. Amalesh et al. compared different channel heat sinks, where zigzag and round slot channels showed excellent cooling performance [31]. Dai et al. studied the cooling performance

difference between straight channels and equivalent corrugated channels, and the results showed that although the heat transfer ability of corrugated channels was greatly improved, it caused a larger loss of pressure drop [32]. Chein et al. studied the effect of different inlet and outlet arrangements on the performance of the radiator and found that the performance of the radiator with the V-shaped inlet and outlet layout was the best [33]. Several studies have shown that bifurcated tree-like channels have better temperature uniformity [34-36]. For cooling flow channels, the influence of parameters such as flow channel cross-sectional shape and wavelength on cooling performance has been studied by several authors [37-40]. At present, most of the active phased array radar T/R modules use liquid cooling systems. The liquid cooling system is mainly composed of connecting pipes, pumps, cold plates and other components[6]. The cold plate is the core part of the cooling system because its flow channel will play a decisive role in the cooling performance of the cooling system. A liquid cold plate (LCP) is a typical indirect cooling device [41, 42]. The cold plate and the module base plate are connected by bolts. Therefore, the coolant flows in the cold plate without direct contact with the electronic components [43-45]. The outer surface of the cold plate is loaded with various electronic components, and the heat generated by the electronic components during operation is taken away by the cooling medium passing through the internal flow channel of the cold plate, thereby achieving the purpose of cooling. With the rise of machining level, the flow channels inside the cold plate are no longer limited to a single straight type and hollow groove type. These structures have the problems of insufficient heat dissipation capacity and uneven air distribution [46, 47]. The common flow channel forms of liquid cooling plates are straight channels and serpentine channels. At present, the research on the cold plate in China and abroad mainly focuses on the optimization and improvement of the existing channel structure, and the exploration of the new channel structure is less [48].

In this paper, the T/R module is taken as the research object, and four different flow channel types of cooling plates are designed, including an S-type channel, Z-type channel, mosaic channel and double-layer channel, and the influence of fluid flow rate, coolant temperature and different coolants on the performance of the cooling plate is studied by simulation software. This study is expected to provide researchers and engineers with a design method for cooling plates for electronic components and provide technical support for thermal management for engineering applications. Ultimately, this will help decrease electronic pollution and contribute to environmental protection [49-51].

2. Structure and design

T/R module is widely used in active phased array radar. It is mainly used to amplify the transmitted signal, amplify the received signal and control the amplitude and phase of the signal. It is composed of the attenuator, phase shifter, power amplifier and other microwave components. This reference gave a detailed introduction to the T/R module [52]. According to the relevant prediction, the heat flux of the phased array T/R module will exceed 1000 W/cm2 in the future, so it is an electronic component with high requirements for heat dissipation.

A liquid cooling plate's ability to transmit heat is influenced by a number of competing parameters, including the heat transfer area, flow rate, volume, and weight of the plate. In general, the complex flow channel structure serves to increase the bypass, which facilitates the heat transfer between the liquid and the cold plate wall. However, this also leads to an increased pressure drop in the flow path. The structure of the flow channel or even the cold plate will be harmed if the pressure in

the flow channel is too high and the wall of the cold plate is too thin. For practical engineering applications, designing a flow channel cold plate structure that can boost heat transfer while preventing an excessive pressure drop is crucial.

The design is based on the principle of minimum volume and mass, with the T/R modules (heat sources) symmetrically distributed on the front and back of the cold plate. As shown in Fig. 1, the liquid cooling plate involved in this paper is mainly used to cool 16 T/R modules (25×25×1 mm) mounted symmetrically on the front and rear sides of the cooling plate. The surface of the heat source cannot exceed 70 °C, with a maximum temperature difference of 5 °C between adjacent components. In this paper, aluminum is selected as the cold plate material. To ensure the temperature rise and temperature uniformity of the cold plate, a parallel flow channel structure is used in this thermal design to reduce the pressure resistance. Under the condition of ensuring the temperature rise and temperature uniformity of the cold plate, four new flow channel structures are designed as shown in Fig. 2. The cold plate length, height and thickness are 500 mm, 200 mm and 10 mm respectively. Fig. 2a is an S-type flow channel cold plate; Fig. 2b is a Z - type flow channel cold plate; Fig. 2c is a mosaic structure flow channel cold plate; Fig. 2d is a double-layer channel cold plate.

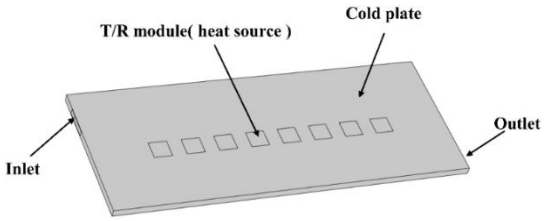

Fig.1 Three-dimensional model of liquid cooling plate.

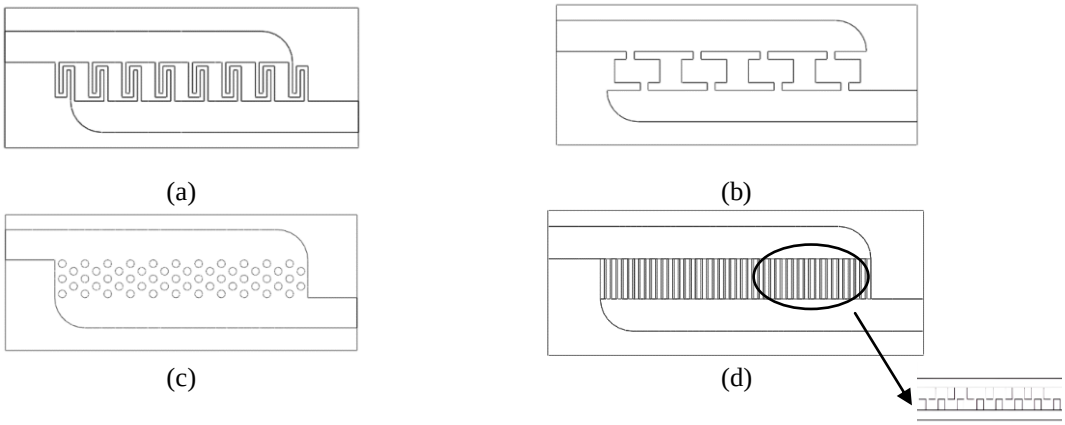

Fig.2 (a) S-type flow channel; (b) Z-shaped flow channel; (c) Mosaic flow Channel; (d) Double flow channel（Enlarged view of flow Channel）.

3. Numerical model

3.1. Model assumptions

In the study, a geometric model is designed and the rounded corners on the cold plate were corrected to reduce the influencing factors. Pressure-velocity coupling is achieved using a coupled algorithm. After updating the properties of the solid and the fluid, the coupled algorithm first solves

the coupling equation consisting of the momentum equation and the continuity equation. Then, use the current value of the solution variable to solve the energy equation. These solution steps are iterated until the convergence criteria are satisfied.

To reduce the complexity of numerical simulations, the following assumptions need to be made when numerical methods are used for simulation analysis:

(1) The fluid is an incompressible Newtonian fluid;

(2) The material of the cooling plate is uniform and the heat transfer coefficient is constant;

(3) The relative velocity between solid surface and fluid is zero, which satisfies the velocity boundary condition without slip;

(4) The heat generated in the T/R module is uniform;

(5) The effects of gravity and other forms of external forces are ignored.

3.2. Conservation equations

The following equation can be obtained according to the physical conservation law followed by the coolant. The continuity equation can be expressed as follow:

$$\frac{\partial \rho}{\partial t} + \rho \nabla \cdot u = 0 \tag{1}$$

where t is the time; u is the fluid velocity vector. ρ is the fluid density.

The momentum equation of the flow field is as follows:

$$\rho\left[\frac{\partial u}{\partial t} + \nabla \cdot (uu)\right] = -\nabla p + \mu \nabla^2 u \tag{2}$$

where P is the pressure; μ is the fluid dynamic viscosity.

The energy equation for the fluid is as follows:

$$\rho c_p \left[\frac{\partial T}{\partial \mathrm{t}} + \nabla \cdot (u \mathrm{T}_l)\right] = k_f \nabla^2 T_l \tag{3}$$

where T_l is the temperature of the coolant liquid; k_f is the thermal conductivity of the coolant liquid. c_P is the fluid-specific heat capacity.

Due to the fluid-solid coupled heat transfer problem, the conservation of energy in solid media needs to satisfy the following equation:

$$\rho_s c_{p,s} \frac{\partial T}{\partial t} = k_s \nabla^2 T_l \tag{4}$$

where ρ_s is the solid density, $c_{p,s}$ is the solid specific heat capacity, and k_s is the solid thermal conductivity.

3.3. Boundary conditions

Heat transfer is a complex process, and there are too many factors that affect its performance, it is difficult to evaluate the cooling effect of coolant through a single standard. This paper analyzes the heat dissipation performance of the cold plate under certain working conditions. The T/R module is placed on the surface of the cold plate and a thermally conductive silicone grease with a thermal resistance of 0.3 °C/W is used, evenly distributed above the runners to better transfer heat. The power

of a single heat source module is 10 W, and the total power is 160 W. If the working module is directly placed in the air without a cold plate to cool down and dissipate heat, its temperature can rise above 100 °C. The coolant inlet temperature is 25 °C, the inlet flow velocity is 1 m/s, and the allowable inlet and outlet pressure difference of the circulating water pump is 0.3 MPa.

3.4. Grid independence verification

The use of SOLIDWORKS to save the liquid-cooled plate and T/R module as IGS format output and import into ICEPAK. ICEPAK uses the FLUENT computational fluid dynamics (CFD) solution engine, which applies the finite volume method for fast solution of both structured and unstructured meshes. The effect of the number of grids on the numerical results of this model was analyzed by testing the independence of the grids. Fig. 3(a) shows the relationship between the number of grids and the maximum temperature of the cold plate at the same flow rate. In this paper, ortho-hexahedral meshing is used. It can be found that the maximum temperature of the cold plate increases by 0.01 % for grid 3015689 compared to grid 1767479, and the error is small enough to consider that the grid does not affect the results. Therefore, the number of grids chosen for all numerical analyses is 1767479. In addition, independent tests of time steps were conducted, and in this paper, a time step of 1s was chosen considering the computational cost, as shown in Fig. 3(b). In the process of iteration, the residual values of each physical quantity reach the convergence criteria and the computation will be judged to be converged.

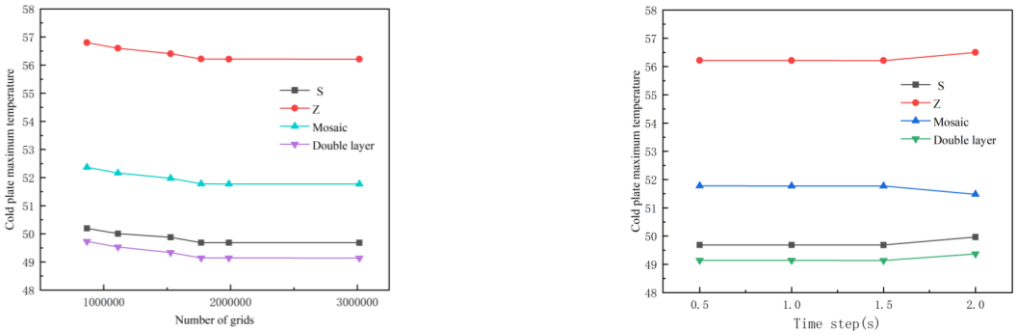

(a) **(b)**

Fig.3. Independent test: (a) grid number (b) time step.

4. Results and discussion

4.1. Model verification

To verify the simulation results, the fluid flow and heat transfer in the cooling plate of the T/R module were numerically simulated. At the same operating conditions, the simulation results were compared with the results of Baek et al. [53]. The simulation results are compared with the reference data, as shown in Fig. 4. It can be seen that the results of the present simulation are in good agreement with the numerical simulation results in the literature [53]. The maximum difference between results is less than 5 %.

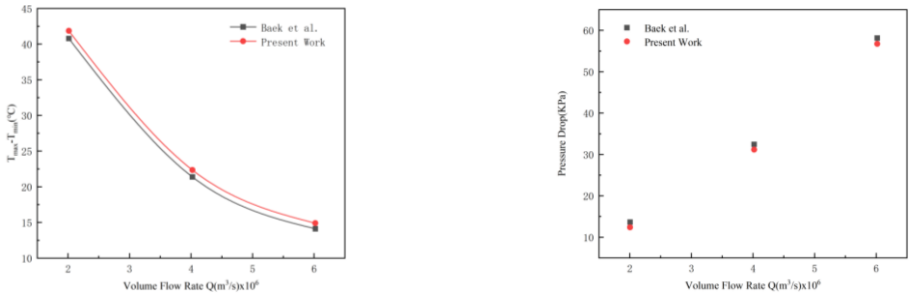

(**a**) (**b**)

Fig.4. Model verification: (a) Maximum temperature difference at different flow rate. (b) Pressure drop at different flow rate.

4.2. Performance comparison

4.2.1. Temperature distribution

The temperature distribution of the cold plate under the same working conditions in the four flow channels is shown in Fig. 5. It can be shown in the figure that the highest temperature area of the S-type flow channel cold plate is distributed near the outlet and the lowest temperature area is distributed near the inlet. On the contrary, the highest temperature of the mosaic flow channel is distributed at the inlet and the lowest temperature is distributed at the outlet. The temperature distributions of the Z-type and double-layer flow channels are similar, with the highest temperatures occurring in the middle area of the cold plate. The difference in temperature distribution is related to the four flow channel structures. The fluid flow in the S-shaped flow channel is constant, and the cold fluid flows into the flow channel, which continuously absorbs the heat emitted by the heat source during the flow process, so that the temperature of the fluid continues to rise. When the fluid enters the mosaic flow channel, initially due to the excessive flow velocity, the flow distribution at the inlet is uneven, resulting in less coolant flowing through the heat source and poor heat dissipation. Although the structure of the Z-type flow channel and the S-type flow channel are similar, the amount of heat dissipation is also different due to the difference in the time that the coolant flows through the heat source. In terms of heat dissipation, the double-layer flow channel cold plate is more effective than the other three flow channel cold plates.

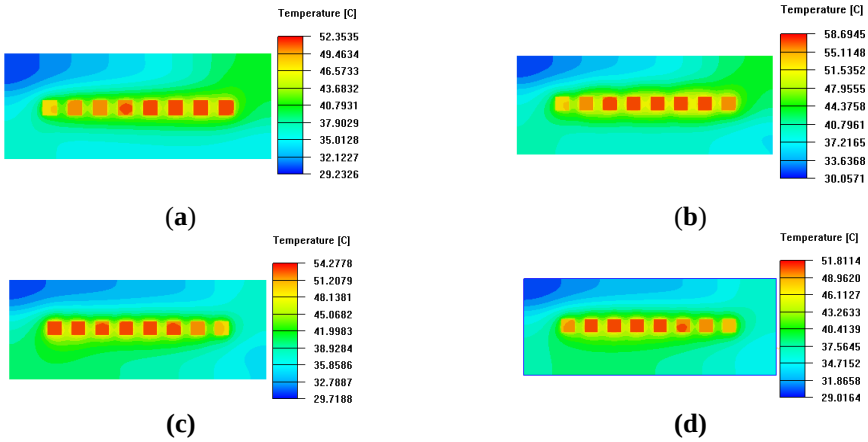

Fig.5. Temperature clouds of cold plate with different flow channels: (a) S-type flow channel; (b) Z-shaped flow channel; (c) Mosaic flow Channel; (d) Double flow channel.

4.2.2. Pressure distribution

Fig. 6 shows the pressure distribution of the four flow channel cold plates. It can be seen that the S-type flow channel cooling plate has the largest pressure drop. Conversely, the mosaic flow channel cooling plate has the smallest pressure drop. Therefore the mosaic flow channel has lower internal energy loss. The pressure drop of the S-type flow channel cooling plate is 51.1 %, 282.7 %, and 203.6 % larger than that of the Z-type flow channel cooling plate, the mosaic flow channel cooling plate, and the double-layer flow channel cooling plate, respectively. There is a strong correlation between pressure distribution and velocity distribution, and this relationship conforms to Bernoulli law [54]. In the comparison of this index, the mosaic-type cooling plate performs the best, and conversely the S-type flow channel cooling plate performs the worst. The S-type flow channel cooling plate blocks the coolant to a greater extent, while the mosaic flow channel effectively reduces the blockage of the coolant and reduces the energy loss.

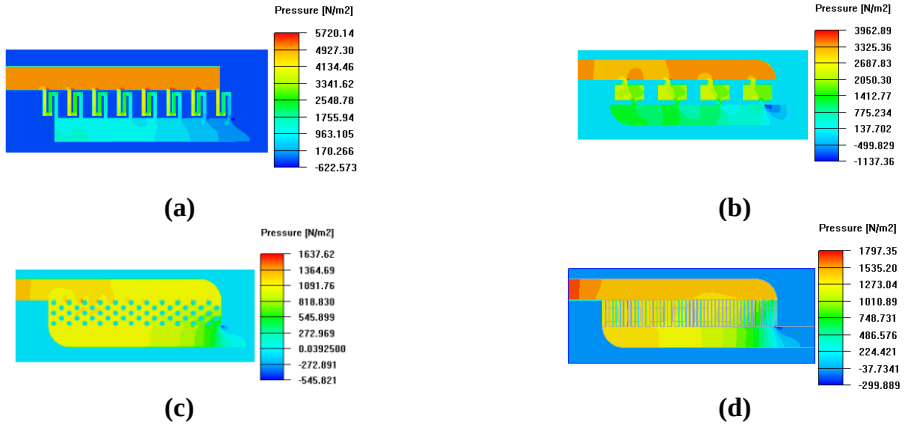

Fig.6. Pressure cloud diagram of the cold plate with different flow channels: (a) S-type flow channel; (b) Z-shaped flow channel; (c) Mosaic flow Channel; (d) Double flow channel.

4.3. Influence of working conditions

4.3.1. Influence of fluid inlet velocity.

Fig. 7 shows the relationship between the maximum temperature of the cold plate at different inlet flows, the outlet temperature and the pressure loss of the cold plate in each flow field. From Fig 7 (a) (b), it can be seen that when the inlet temperature is constant, the maximum temperature of the cold plate and the outlet temperature of the cold plate decrease with the increase of the flow velocity. At the flow velocity of 0.6 m/s, the maximum temperature and outlet temperature of the double-layer flow channel cold plate were 9.19 ℃ and 5.97 ℃ lower than those of the z-type cold plate. As the flow velocity increases, the advantage in heat removal weakens, and the difference between the four flow channels decreases. Therefore, increasing the flow rate of coolant can improve the heat transfer capacity of the cooling plate, but it is better to choose the appropriate flow velocity.

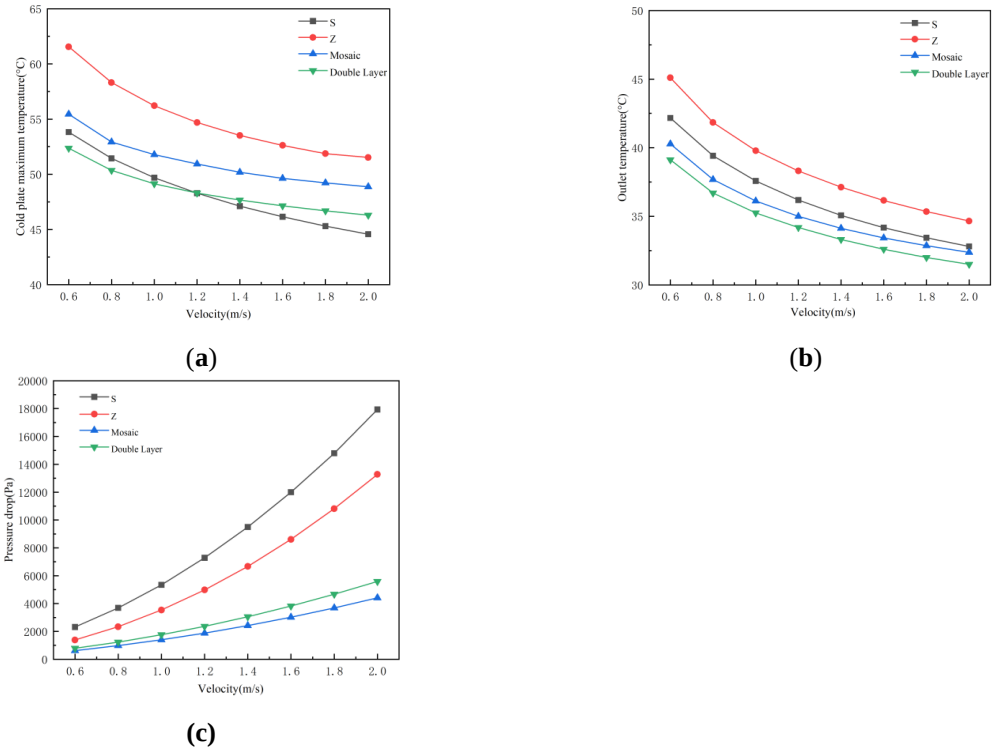

Fig.7. Effect of inlet velocity on the performance of cooling plates: (a) Cold plate maximum temperature; (b) Outlet temperature; (c) Pressure drop.

It can be seen from Fig. 7(c) that when the flow velocity changes from 0.6 m/s to 2.0 m/s, the resistance loss of the S-type flow channel cold plate is relatively large, and the growth trend is very obvious, and the maximum change value of the pressure drop is 15623.23 Pa. The Z-shaped flow channel growth trend is also apparent. The pressure loss of the mosaic flow channel and the double-layer flow channel has a small change, and the trend is relatively gentle. By increasing the fluid flow rate, the convection heat transfer coefficient of the flow channel wall will increase, the coolant can take away more heat, and the temperature will decrease, but at the same time, the pressure loss will increase. The S-type flow channel cold plate consumes more energy, while the mosaic flow channel

and double-layer flow channel consume less energy, so their cost is also smaller, especially at higher flow rates. It can be seen that the greater the inlet velocity of fluid is not the better, and the cooling efficiency and pressure loss should be taken into account to select an optimal value.

4.3.2. Influence of fluid inlet temperature

As shown in Fig. 8, the effect of fluid inlet temperature on the performance of the cold plate was studied. When the inlet temperature is 20 ℃, the maximum temperatures of S-type flow channel, Z-type flow channel, mosaic flow channel and double layer flow channel cold plate are 44.7 ℃, 51.3 ℃, 46.7 ℃ and 44.2 ℃, respectively. As can be seen from Fig. 8, when the flow velocity is kept constant, the maximum temperature of the cold plate and the outlet temperature of the cold plate both increase gradually with the increase of the fluid inlet temperature. The comparison results of the four flow channels show that although the changing trend is the same, the S-type flow channel and double-layer flow channel have better heat dissipation performance, the mosaic flow channel is the second and the Z-type flow channel is the worst. At an inlet temperature of 30 °C, the outlet temperature of the double-layer flow channel is 34.8 % lower than that of the Z-type flow channel. Fig. 8(c) shows that a change in fluid inlet temperature has little effect on the pressure drop of the cold plate. The fluid flows in the cold plate, generating a pressure loss along the way.

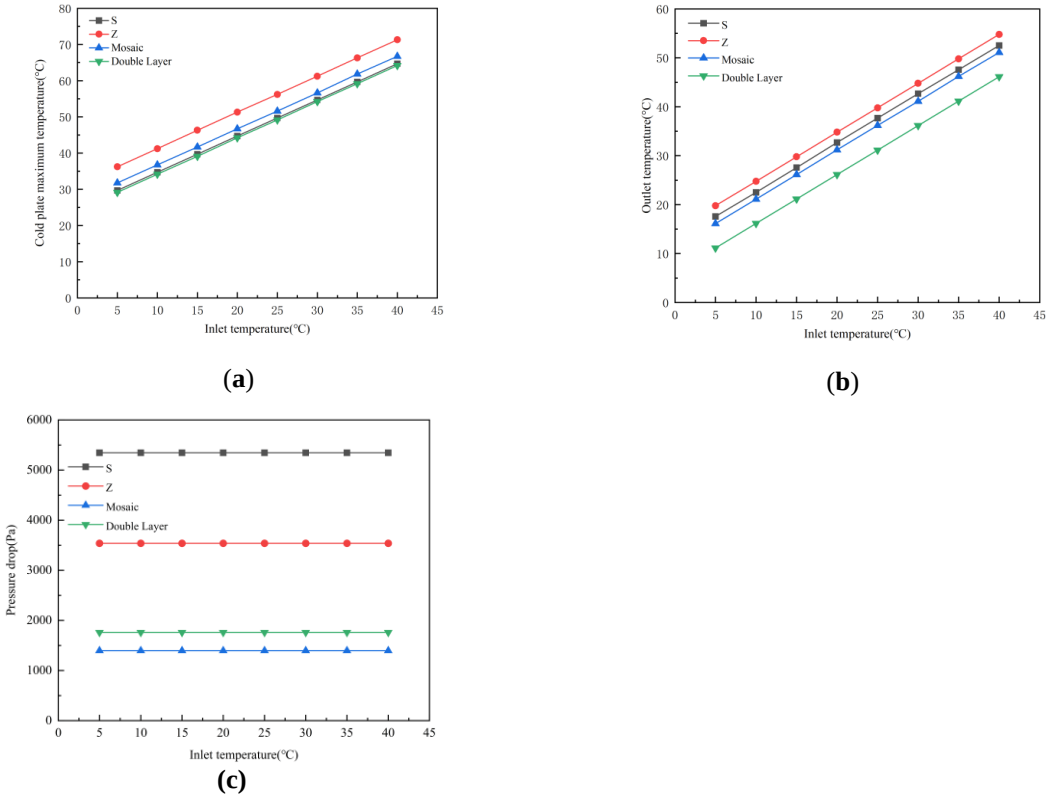

Fig.8. Effect of inlet temperature on the performance of cooling plates. (a) Cold plate maximum temperature; (b) Outlet temperature; (c) Pressure drop.

4.3.3. Influence of changing the coolant

Different coolants have different physical parameters, so they have different effects on the cooling effect. When T/R modules operate below 0 °C, water as a coolant is prone to freezing, which affects the cooling effect, so it is necessary to study new coolants to dissipate heat for T/R modules in low-temperature environments.

The physical properties of different coolants are also different, and the thermal conductivity of the coolant directly affects the cooling effect. At the same time, the kinematic viscosity of different coolants is also different, which makes the flow state in the flow channel different, resulting in the change of the convective heat transfer coefficient, and the heat taken away when passing through the same area is also different, so the heat dissipation performance is different. As shown in Fig. 9, when the coolant is water, there is little difference in the thermal performance of the four flow channels; When the cooling liquid is an ethylene glycol-aqueous solution, with the increase of ethylene glycol concentration, the difference in heat dissipation performance of the four flow channels becomes larger and larger. The reason for this phenomenon is the large difference in heat dissipation between the cold plates of different flow channels. When the coolant in the double-layer flow channel is the 20 % glycol-water solution, the maximum temperature of the cold plate is 2.13 % lower than when the coolant is water. Fig. 9(c) shows that the effect of the cooling liquid on the pressure drop of the cold plate is very large and the trend is very obvious, which is due to the difference in the cooling liquid density. The higher the density of coolant, the higher the pressure drop of the cold plate.

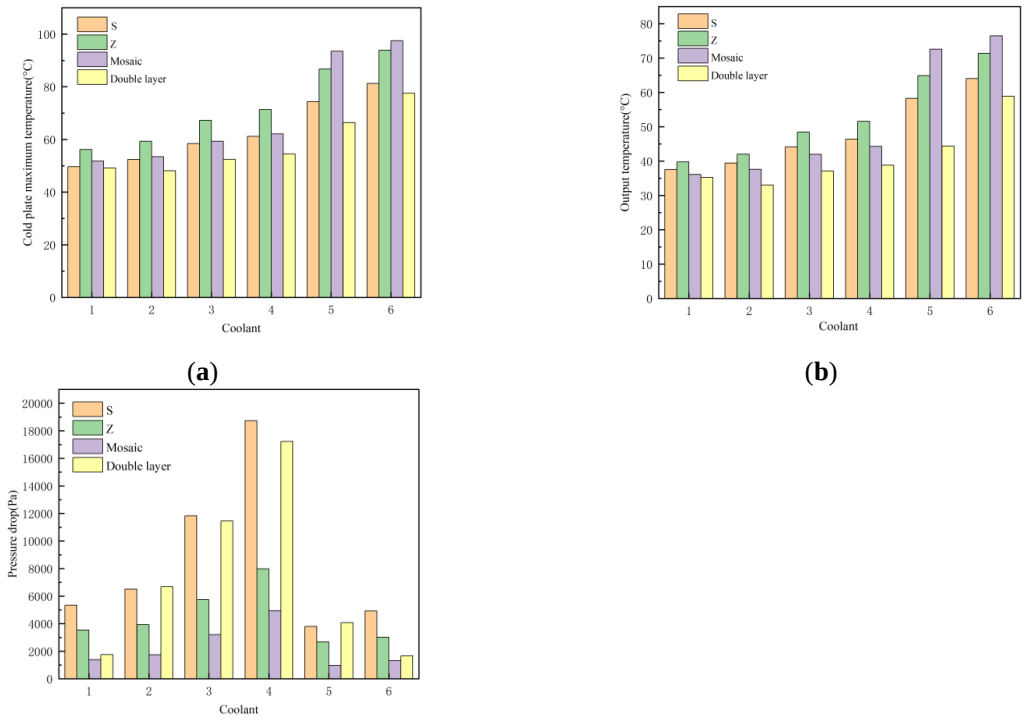

Fig.9. Effect of coolant on the performance of cooling plates. (a) Cold plate maximum temperature; (b) Outlet temperature; (c) Pressure drop. ((Remarks: Coolant 1. water 2. 20% ethylene glycol - water solution 3. 60% ethylene glycol - water solution 4. 80% ethylene glycol - water solution 5. methanol 6. ethanol).

5. Conclusion

To reduce the maximum temperature and local temperature difference of high heat flux electronics, four novel flow channel cooling plates were designed in this study. This paper takes the T/R module as the research object and compares the temperature and pressure distribution of four cold plates through numerical simulation. Furthermore, the comprehensive performance of four cold plates was compared and discussed under varying inlet velocities, fluid temperatures, and coolants. The main conclusions are summarized as follows:

(1) With the same thermal management requirements, the flow channel structure has a significant effect on the cooling effect of the cold plate. The average temperature of the cold plate using the double-layer flow channel is the lowest, and the average temperature of the cold plate using the Z-type flow channel is the highest. The results show that the maximum temperature of the cold plate of the double-layer flow channel is 6.88 °C lower than that of the Z-type flow channel. The mosaic flow channel cold plate pressure drop is the lowest, and the pressure drop of the mosaic flow channel design is 1.396 kPa, which is 73.87 % lower than that of the Z-type flow channel design.

(2) Increasing the flow velocity improved the cooling performance of the four flow channels cold plate most significantly. When the flow velocity increased from 0.6 m/s to 1.2 m/s, the maximum temperature drop of the cold plate was 11.15 % of that of the Z-type flow channel cold plate. However, this increased the pressure drop of the Z-type flow channel cooling plate. Lowering the coolant inlet temperature can improve the cooling performance of the cold plate.

(3) The cooling effect of the double layer flow channel cold plate is the best when the coolant is 20 % ethylene glycol - water solution, which is 1.05 °C lower than the maximum temperature of the cold plate when the coolant is water, and the cooling effect is best when the coolant of the remaining three flow channel cold plates is water. Due to cost constraints in practical applications, the cooling liquid should be selected comprehensively considering the heat dissipation performance and cost.

In summary, the double-layer flow channel cold plate mechanism has uniform temperature distribution, the best cooling performance and the greatest potential. The simulation results will provide a reference for the design of thermal management systems for high heat flux electronics.

Acknowledgment

We gratefully acknowledge the financial support of the Scientific Research Foundation of Nanjing Forestry University (No. GXL2018004).

Nomenclature

Roman letters

t -time [s]

u - fluid velocity vector [$m.s^{-1}$]

P - pressure [Pa]

T - temperature [K]

k_f - thermal conductivity of the coolant liquid [$\mathrm{W \cdot m^{-1} \cdot K^{-1}}$]

k_s - thermal conductivity of the solid [$\mathrm{W \cdot m^{-1} \cdot K^{-1}}$]

Greek letters

ρ - density [$kg.m^{-3}$]

μ - viscosity [$kg.m^{-1}.s^{-1}$]

C_P - fluid-specific heat capacity [$\mathrm{J \cdot kg^{-1} \cdot K^{-1}}$]

$C_{p,s}$ - solid specific heat capacity [$\mathrm{J \cdot kg^{-1} \cdot K^{-1}}$]

References

[1] He, X., *et al.*, Temperature, precipitation and runoff prediction in the Yangtze River Basin based on CMIP 6 multi-model, *J. Nanjing For. Univ. Nat. Sci. Ed.* (2022), pp. 1-10, DOI No. 10.12302/j.issn.1000-2006.202203028

[2] Wang, L., *et al.*, Molecular dynamics mechanism of metal salt hydrate-based deep eutectic solvent to dissolve cellulose at room temperature, *J. For. Eng.*, *7*. (2022), 04, pp. 64-71, DOI No. 10.13360/j.issn.2096-1359.202112025

[3] Jiang, X., *et al.*, Evaluating the Carbon Emissions Efficiency of the Logistics Industry Based on a Super-SBM Model and the Malmquist Index from a Strong Transportation Strategy Perspective in China, *International Journal of Environmental Research and Public Health*, *17*. (2020), 22, DOI No. 10.3390/ijerph17228459

[4] Yao, N., *et al.*, Analysis of carbon sequestration effect of sloping land conversion program in Loess Plateau from the perspective of slope, *J. Nanjing For. Univ. Nat. Sci. Ed.* (2022), pp. 1-17, DOI No. 10.12302/J.ISSN.1000-2006. 202111033

[5] Zou, X., *et al.*, Mechanisms and methods for augmenting carbon sink in forestry, *J. Nanjing For. Univ. Nat. Sci. Ed.* (2022), pp. 1-12, DOI No. 10.12302/j.issn.1000-2006.202209008

[6] Qian, S., *et al.*, Topology optimization of fluid flow channel in cold plate for active phased array antenna, *Structural and Multidisciplinary Optimization*, *57*. (2018), 6, pp. 2223-2232, DOI No. 10.1007/s00158-017-1852-8

[7] Liang, J.-Y., *et al.*, Design of an Integrated Heat Dissipation Mechanism for a Quad Transmit Receive Module of Array Radar, *Applied Sciences-Basel*, *11*. (2021), 15, DOI No. 10.3390/app11157054

[8] Sonne, -.C., *et al.*, - Is engineered wood China's way to carbon neutrality?, - *Journal of Bioresources and Bioproducts*, - *7*. (2022), - 2, pp. - 83, DOI No. - 10.1016/j.jobab.2022.03.001

[9] Peng, H., *et al.*, A review of the value realization path of forestry carbon sink products, *J. Nanjing For. Univ. Nat. Sci. Ed.* (2022), pp. 1-12, DOI No. 10.12302/j.issn.1000-2006.202207023

[10] Liu, J.,Z. Lin, Energy and Exergy Performances of Floor, Ceiling, Wall Radiator and Stratum Ventilation Heating Systems for Residential Buildings, *Energy and Buildings*, *220*. (2020), DOI No. 10.1016/j.enbuild.2020.110046

[11] Sun, S., A new stress field intensity model and its application in component high cycle fatigue research, *Plos One*, *15*. (2020), 7, DOI No. 10.1371/journal.pone.0235323

[12] Xu, X., *et al.*, Active Control on Path Following and Lateral Stability for Truck-Trailer Combinations, *Arabian Journal for Science and Engineering*, *44*. (2019), 2, pp. 1365-1377, DOI No. 10.1007/s13369-018-3527-1

[13] Scott, M., *et al. Sampson MFR active phased array antenna*,IEEE International Symposium on Phased Array Systems and Technology,Boston, Ma,2003, pp. 119-123

[14] Hoft, D.J., Solid State Transmit/Receive Module for the PAVE PAWS (AN/FPS-115) Phased Array RADAR, *1978 IEEE-MTT-S International Microwave Symposium Digest*. (1978),

[15] Whicker, L.R., Active phased array technology using coplanar packaging technology, *IEEE Transactions on Antennas and Propagation*, *43*. (1995), 9, pp. 949-952

[16] Nakagawa, M., *et al. Development of Thermal Control for Phased Array Antenna*,International Communications Satellite Systems Conference & Exhibit,2003,

[17] Obey, -.G., *et al.*, - Biochar derived from non-customized matamba fruit shell as an adsorbent for wastewater treatment, - *Journal of Bioresources and Bioproducts*, - *7*. (2022), - 2, pp. - 109, DOI No. - 10.1016/j.jobab.2021.12.001

[18] Cheng, Z.,Z. Lu, Research on Dynamic Load Characteristics of Advanced Variable Speed Drive System for Agricultural Machinery during Engagement, *Agriculture-Basel*, *12*. (2022),

2, DOI No. 10.3390/agriculture12020161
[19] Li, B.L.,L. Zeng, Fractional Calculus Control of Road Vehicle Lateral Stability after a Tire Blowout, *Mechanika*, *27*. (2021), 6, pp. 475-482, DOI No. 10.5755/j02.mech.28524
[20] Chai, X.Y., *et al.*, Development and Experimental Analysis of a Fuzzy Grey Control System on Rapeseed Cleaning Loss, *Electronics*, *9*. (2020), 11, DOI No. 10.3390/electronics9111764
[21] Agrawal, A.K., *et al. An active phased array antenna packaging scheme*,Antennas and Propagation Society International Symposium, 1996. AP-S. Digest,1996,
[22] Narvaez, J.A., *et al.*, Computational modeling of a microchannel cold plate: Pressure, velocity, and temperature profiles, *International Journal of Heat and Mass Transfer*, *78*. (2014), pp. 90-98, DOI No. 10.1016/j.ijheatmasstransfer.2014.06.006
[23] Tian, J., *et al.*, Differential Steering Control of Four-Wheel Independent-Drive Electric Vehicles, *Energies*, *11*. (2018), 11, DOI No. 10.3390/en11112892
[24] Schmidt, R.R.,B.D. Notohardjono, High-end server low-temperature cooling, *Ibm Journal of Research and Development*, *46*. (2002), 6, pp. 739-751, DOI No. 10.1147/rd.466.0739
[25] Esmaili, Q., *et al.*, Experimental analysis of heat transfer in ribbed microchannel, *International Journal of Thermal Sciences*, *130*. (2018), pp. 140-147, DOI No. 10.1016/j.ijthermalsci.2018.04.020
[26] Zhang, Y.P., *et al.*, Thermal performance study of integrated cold plate with power module, *Applied Thermal Engineering*, *29*. (2009), 17-18, pp. 3568-3573, DOI No. 10.1016/j.applthermaleng.2009.06.013
[27] Leng, C., *et al.*, Multi-parameter optimization of flow and heat transfer for a novel double-layered microchannel heat sink, *International Journal of Heat and Mass Transfer*, *84*. (2015), pp. 359-369, DOI No. 10.1016/j.ijheatmasstransfer.2015.01.040
[28] Leng, C., *et al.*, Optimization of thermal resistance and bottom wall temperature uniformity for double-layered microchannel heat sink, *Energy Conversion and Management*, *93*. (2015), pp. 141-150, DOI No. 10.1016/j.enconman.2015.01.004
[29] Leng, C., *et al.*, An improved design of double-layered microchannel heat sink with truncated top channels, *Applied Thermal Engineering*, *79*. (2015), pp. 54-62, DOI No. 10.1016/j.applthermaleng.2015.01.015
[30] Vinoth, R.,D.S. Kumar, Channel cross section effect on heat transfer performance of oblique finned microchannel heat sink, *International Communications in Heat and Mass Transfer*, *87*. (2017), pp. 270-276, DOI No. 10.1016/j.icheatmasstransfer.2017.03.016
[31] Amalesh, T.,N.L. Narasimhan, Introducing new designs of minichannel cold plates for the cooling of Lithium-ion batteries, *Journal of Power Sources*, *479*. (2020), DOI No. 10.1016/j.jpowsour.2020.228775
[32] Dai, Z., *et al.*, Impact of tortuous geometry on laminar flow heat transfer in microchannels, *International Journal of Heat and Mass Transfer*, *83*. (2015), pp. 382-398, DOI No. 10.1016/j.ijheatmasstransfer.2014.12.019
[33] Chein, R.,J. Chen, Numerical study of the inlet/outlet arrangement effect on microchannel heat sink performance, *International Journal of Thermal Sciences*, *48*. (2009), 8, pp. 1627-1638, DOI No. 10.1016/j.ijthermalsci.2008.12.019
[34] Xia, C., *et al.*, Conjugate heat transfer in fractal tree-like channels network heat sink for high-speed motorized spindle cooling, *Applied Thermal Engineering*, *90*. (2015), pp. 1032-1042, DOI No. 10.1016/j.applthermaleng.2015.07.024
[35] Yu, X.-f., *et al.*, A study on the hydraulic and thermal characteristics in fractal tree-like microchannels by numerical and experimental methods, *International Journal of Heat and Mass Transfer*, *55*. (2012), 25-26, pp. 7499-7507, DOI No. 10.1016/j.ijheatmasstransfer.2012.07.050
[36] Escher, W., *et al.*, Efficiency of optimized bifurcating tree-like and parallel microchannel networks in the cooling of electronics, *International Journal of Heat and Mass Transfer*, *52*. (2009), 5-6, pp. 1421-1430, DOI No. 10.1016/j.ijheatmasstransfer.2008.07.048
[37] Lin, L., *et al.*, Heat transfer enhancement in microchannel heat sink by wavy channel with

changing wavelength/amplitude, *International Journal of Thermal Sciences*, *118*. (2017), pp. 423-434, DOI No. 10.1016/j.ijthermalsci.2017.05.013
[38] Zhou, J., *et al.*, Design of microchannel heat sink with wavy channel and its time-efficient optimization with combined RSM and FVM methods, *International Journal of Heat and Mass Transfer*, *103*. (2016), pp. 715-724, DOI No. 10.1016/j.ijheatmasstransfer.2016.07.100
[39] Rostami, J., *et al.*, Optimization of conjugate heat transfer in wavy walls microchannels, *Applied Thermal Engineering*, *82*. (2015), pp. 318-328, DOI No. 10.1016/j.applthermaleng.2015.02.069
[40] Sui, Y., *et al.*, An experimental study of flow friction and heat transfer in wavy microchannels with rectangular cross section, *International Journal of Thermal Sciences*, *50*. (2011), 12, pp. 2473-2482, DOI No. 10.1016/j.ijthermalsci.2011.06.017
[41] Shi, M., *et al.*, Thermal performance of insulated gate bipolar transistor module using microchannel cooling base plate, *Applied Thermal Engineering*, *201*. (2022), DOI No. 10.1016/j.applthermaleng.2021.117718
[42] Zhou, W., *et al.*, Review on the Battery Model and SOC Estimation Method, *Processes*, *9*. (2021), 9, DOI No. 10.3390/pr9091685
[43] Lu, Z., *et al.*, Effect of branching level on the performance of constructal theory based Y-shaped liquid cooling heat sink, *Applied Thermal Engineering*, *168*. (2020), DOI No. 10.1016/j.applthermaleng.2019.114824
[44] Sheng, L., *et al.*, Numerical investigation on a lithium ion battery thermal management utilizing a serpentine-channel liquid cooling plate exchanger, *International Journal of Heat and Mass Transfer*, *141*. (2019), pp. 658-668, DOI No. 10.1016/j.ijheatmasstransfer.2019.07.033
[45] Al-Waaly, A.A.Y., *et al.*, Liquid cooling of non -uniform heat flux of a chip circuit by subchannels, *Applied Thermal Engineering*, *115*. (2017), pp. 558-574, DOI No. 10.1016/j.applthermaleng.2016.12.061
[46] Li, W., *et al.*, The ecological restoration technology for lake wetland in the background of carbon peaking and carbon neutrality, *J. Nanjing For. Univ. Nat. Sci. Ed*. (2022), pp. 1-13, DOI No. 10.12302/j.issn.1000-2006.202209031
[47] Huang, S., *et al.*, Research progress of photochemical-based aggregation-induced luminescent materials *J. For. Eng.* (2022), pp. 1-12, DOI No. 10.13360/j.issn.2096-1359.202202008
[48] Chen, F., *et al.*, Topology optimization design and numerical analysis on cold plates for lithium-ion battery thermal management, *International Journal of Heat and Mass Transfer*, *183*. (2022), DOI No. 10.1016/j.ijheatmasstransfer.2021.122087
[49] Lian, C.,Z. Wu, Research progress on environmental characteristics of bamboo materials and its products, *J. For. Eng.*, *7*. (2022), 01, pp. 23-30, DOI No. 10.13360/j.issn.2096-1359.202101016
[50] Nnaemeka, -.I.C., *et al.*, - Optimization and Kinetic Studies for Enzymatic Hydrolysis and Fermentation of Colocynthis Vulgaris Shrad Seeds Shell for Bioethanol Production, - *Journal of Bioresources and Bioproducts*, - *6*. (2021), - 1, pp. - 45, DOI No. - 10.1016/j.jobab.2021.02.004
[51] Wang, W., *et al.*, Preparation and performance of PH sensitive alginate/charcoal slow-release gel spheres *J. For. Eng.*, *7*. (2022), 02, pp. 128-134, DOI No. 10.13360/j.issn.2096-1359.202107014
[52] Tan, M.C., *et al.*, Design and Characterization of T/R Module for Commercial Beamforming Applications, *Ieee Access*, *8*. (2020), pp. 130252-130262, DOI No. 10.1109/access.2020.3009531
[53] Baek, S.M., *et al.*, A numerical study on uniform cooling of large-scale PEMFCs with different coolant flow field designs, *Applied Thermal Engineering*, *31*. (2011), 8-9, pp. 1427-1434, DOI No. 10.1016/j.applthermaleng.2011.01.009
[54] Mo, X., *et al.*, Topology optimization of cooling plates for battery thermal management, *International Journal of Heat and Mass Transfer*, *178*. (2021), DOI No. 10.1016/j.ijheatmasstransfer.2021.121612

Paper submitted: 15.07.2023
Paper revised: 29.09.2023
Paper accepted: 13.10.2023